Supporting Information

In-situ Unravelling Structural Modulation across Charge-Density-Wave Transition in Vanadium Disulfide

Xu Sun [a†], Tao Yao [b†], Zhenpeng Hu [c], Yuqiao Guo [a], Qinghua Liu [b], Shiqiang Wei [b*], Changzheng Wu [a*]

[a] Hefei National Laboratory for Physical Sciences at Microscale, University of Science & Technology of China, Hefei, Anhui, 230026, P.R. China.

[b] National Synchrotron Radiation Laboratory, University of Science and Technology of China, Hefei, 230029, China.

[c] School of Physics, Nankai University, Tianjin, 300071 China.

S 1. Micrograph of the synthesized VS_2.

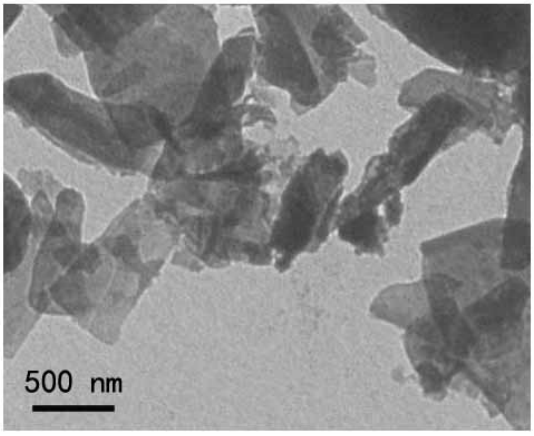

Fig. S1 Transmission electron microscopy (TEM) image of VS_2 sample.

S2. XPS spectra of VS_2.

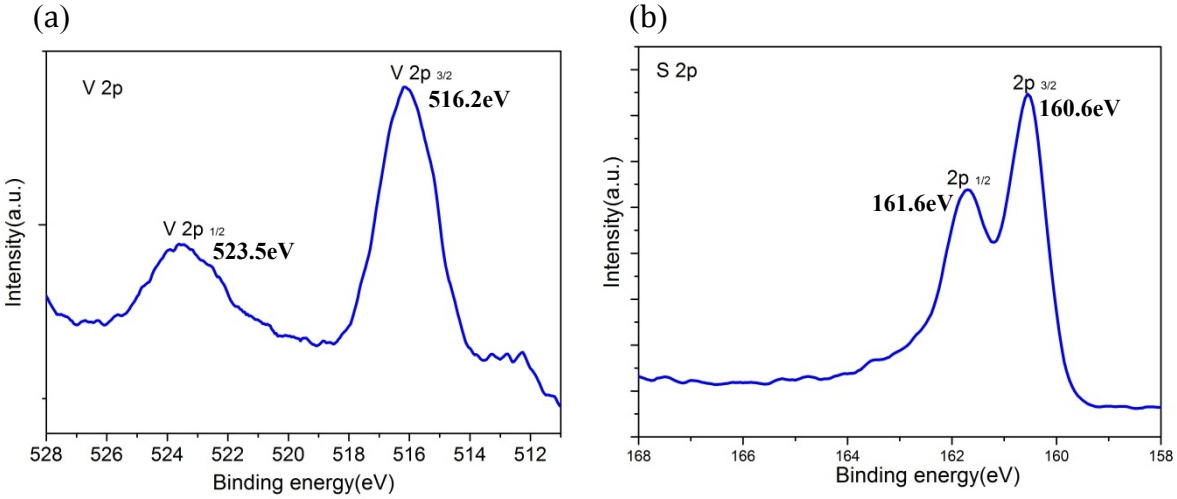

Fig. S2 XPS spectra of the as-synthesized VS_2 sample. The representative energy positions for V2p (a) and S2p (b) are in consistent with the reported value[1,2], demonstrating the formation of pure VS_2 phase.

S3. DSC thermal data of the synthesized VS_2 sample.

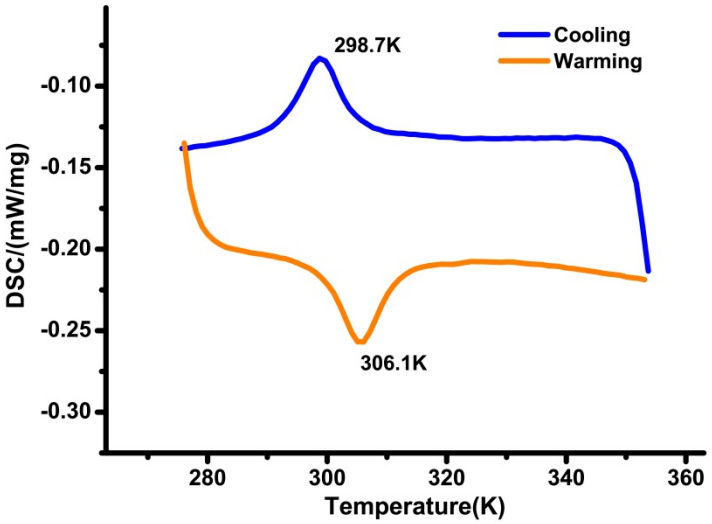

Fig. S3 DSC thermal data of VS_2 sample with the appearance of endothermal peak at 306.1 K (warming curve) and exothermal peak at about 298.7 K (cooling curve), demonstrating the CDW phase transition.

S4. Thermal analyses of VS_2

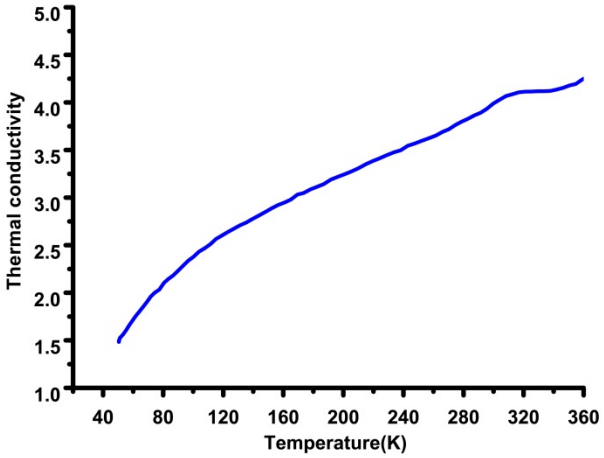

Fig. S4 Temperature-dependent thermal conductivity of VS_2. The inflection points at about 310K demonstrating the CDW phase transition.

S5. Space charge distribution of VS_2

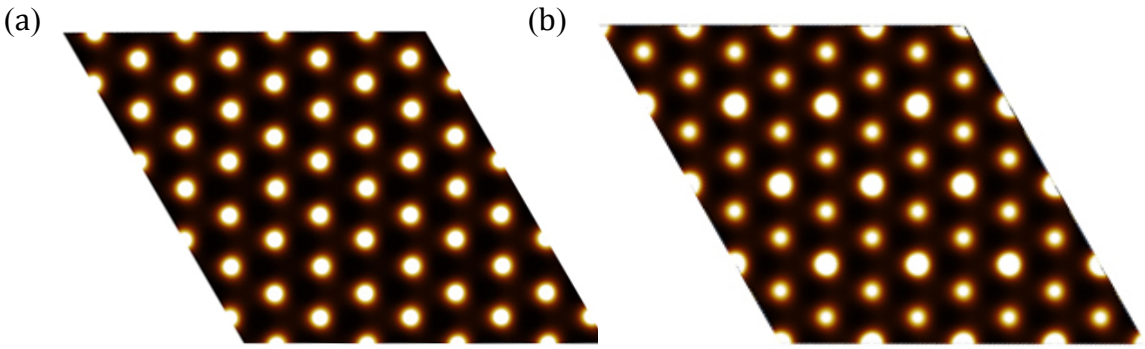

Fig. S5 (a) and (b) The corresponding space charge distribution of VS_2 above and below the transition temperature. They are the local density of states of the a_{1g} band projected above S atoms on one side of VS_2 layer. (a) For the $T > T_{CDW}$ structure, there was a 1×1 periodicity for the bright spots. (b) For the $T < T_{CDW}$ structure, there was a new √3×√3 periodicity for the bright spots.

S6. EXAFS fitting of VS_2 across the CDW transition

Least-squares curve-fittings of the FT peaks for the sample at different temperatures were carried out with the ARTEMIS programs of IFEFFIT.[3] The fittings were done in the *R*-space within the *R*-range of 1.3–3.1 Å. Effective scattering amplitudes and phase-shifts for the V–S and V–V pairs were calculated with the *ab initio* code FEFF8.0.[4] During the curve-fitting, the overall amplitude reduction factor S_0^2 was constrained to the value of 0.78 determined from fitting the reference VS_2 reference. For each coordination pair, the bond length *R* and the Debye–Waller factor σ^2 was allowed to vary. Before the CDW transition at 310 K, we use a single V-V shell for the fitting. And after CDW transition below 280 K, two V-V sub shells were included in the fitting. The satisfactory curve-fitting results are shown in the following **Fig. S6a-d**, and the extracted structural parameters are listed in **Table S1** in the main text.

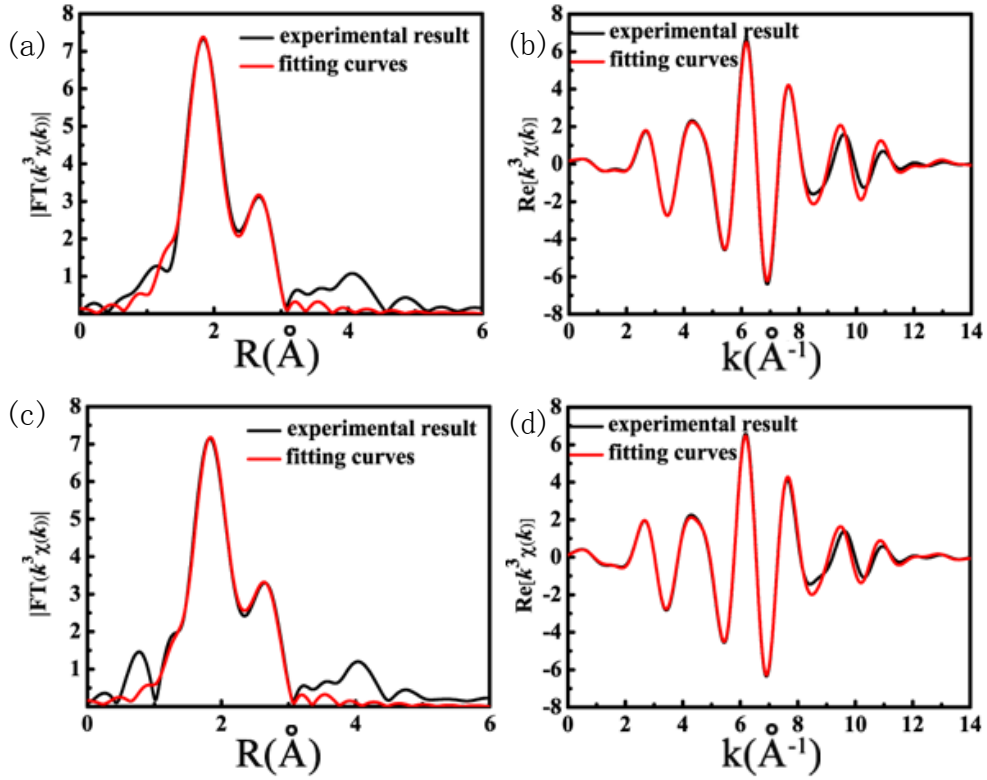

Fig. S6 Single V-V shell fitting curves for q-range (a) and r-range (b) at 310k. Double-shell fitting curves for q-range (c) and r-range (d) at 280k.

In order to check that these fittings are justified, we also carried single V-V shell fitting for the data below 280 K, respectively. The parameters of R-factors and reduced chi-square are summarized in **Table S1**, and the curve-fitting results for 280K are shown in **Fig. S 7a-b**. For the data 280K, the R-factors and reduced chi-square of single V-V shell fitting are much larger than those of two V-V shell fitting. Therefore, fits including two V-V sub shells for the data after CDW transition can permit us to obtain more accurate structural parameters. Besides, the double V-V sub

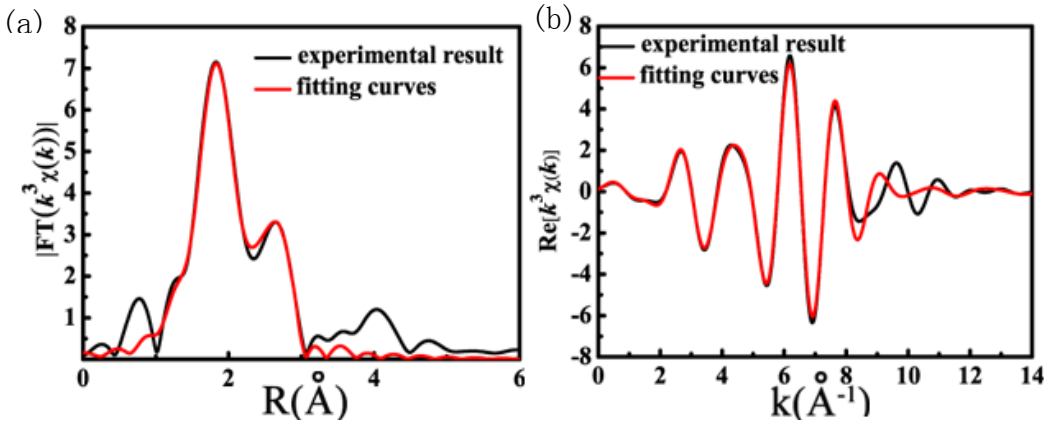

Fig. S7 Single-shell fitting curves for q-range (a) and r-range (b) at 280k.

shells fitting curves at 230K, 150K and 10K were also shown in **Fig. S8**, from which the perfect match of fitting result with the experimental illustrated the availability double V-V shell fitting below the transition temperature.

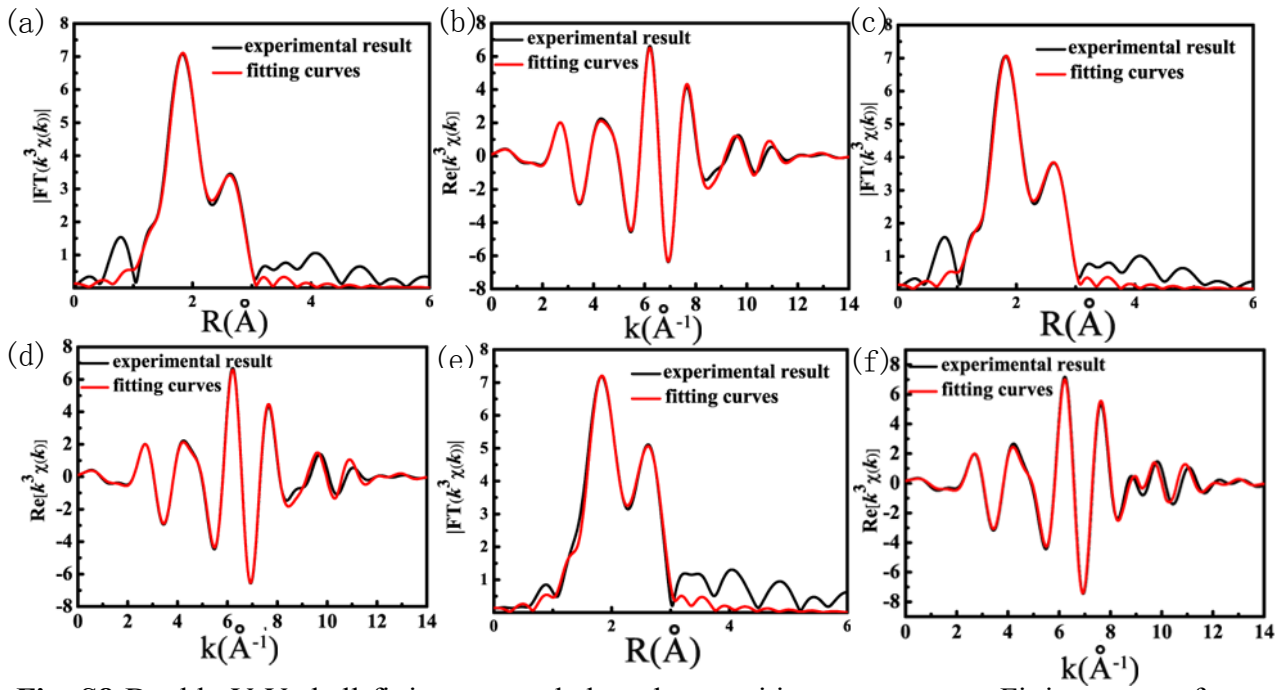

Fig. S8 Double V-V shell fitting curves below the transition temperature. Fitting curves for q-range at 230k (a), 150K (c) and 10K (e). (b), (d) and (f) corresponds to the r-range at 230k, 150Kand 10K, respectively.

Table S1. The structural parameters (distance R, coordination number N, Debye-Waller factor σ^2, Reduced Chi-square and Goodness-of-fit parameter) for the different V–S and V–V pairs for crystalline VS_2 samples at several temperatures during the cooling process. ("SS" and "DS" represent single and two V-V shell fittings, respectively.)

Temperature	Strategy	bond	*R* (Å)	*N*	σ^2 (10^{-3}Å^2)	R-factor	χ_v^2
310 K	SS	V-S	2.34±0.01	6	3.1±0.3	0.002	8.6
		V-V	3.22±0.02	6	5.7±0.5		
280 K	SS	V-S	2.34±0.02	6	2.8±0.3	0.035	37.4
		V-V	3.22±0.02	6	5.3±0.2		
	DS	V-S	2.34±0.02	6	2.9±0.6	0.017	11.2
		V-V	3.11±0.02	1.9±0.2	5.3±0.5		
			3.25±0.01	4.1±0.3			
230 K	SS	V-S	2.34±0.02	6	2.4±0.2	0.057	16.5
		V-V	3.20±0.02	6	5.0±0.2		
	DS	V-S	2.34±0.02	6	2.5±0.2	0.011	9.0
		V-V	3.10±0.02	2.0±0.1	5.1±0.3		
			3.26±0.01	4.0±0.3			
150 K	SS	V-S	2.34±0.02	6	2.0±0.2	0.072	26.2
		V-V	3.20±0.03	6	4.8±0.4		
	DS	V-S	2.34±0.01	6	2.1±0.2	0.007	10.7
		V-V	3.09±0.02	2.0±0.1	4.9±0.5		
			3.26±0.01	4.0±0.2			
10 K	SS	V-S	2.34±0.02	6	1.9±0.2	0.064	22.6
		V-V	3.20±0.03	6	4.5±0.4		
	DS	V-S	2.34±0.02	6	1.9±0.2	0.027	7.6
		V-V	3.08±0.02	2.0±0.1	4.4±0.5		
			3.27±0.01	4.0±0.2			

Reference

(1) C. S. Rout, B.-H. Kim, X. Xu, J. Yang, H. Y. Jeong, D. Odkhuu, N. Park, J. Cho and H. S. Shin, *J. Am. Chem. Soc.* **135**, 8720 (2013).

(2) D. Gao, Q. Xue, X. Mao, W. Wang, Q. Xu and D. Xue, *J. Mater. Chem. C*, **1,** 5909 (2013).

(3) B. Ravel, M. Newville, *J. Synchrotron Rad.* **12**, 537 (2005).

(4) A. L. Ankudinov, B. Ravel, J. J. Rehr, S. D. Conradson. *Phys. Rev. B* **58**, 65 (1998).